METHODS: A Companion to Methods in Enzymology 6, 157–167 (1994)

Kinetics of Receptor and Virus Interaction and Receptor-Induced Virus Disruption: Methods for Study with Surface Plasmon Resonance

José M. Casasnovas,* Robert R. Reed,† and Timothy A. Springer*

*The Center for Blood Research–Harvard Medical School, 200 Longwood Avenue, Boston, Massachusetts 02115; and †Pharmacia Biosensor, 800 Centennial Avenue, Piscataway, New Jersey 08855

We have used BIAcore to analyze the kinetics of the interaction between rhinovirus and soluble intercellular adhesion molecule-1 (sICAM-1). Human rhinovirus serotype 3 (HRV3) was immobilized in the carboxymethylated dextran of the sensor chip, and sICAM-1 expressed with baculovirus was injected through the rhinovirus surface. sICAM-1 bound specifically to HRV3. The virus remained intact in the surface after 12 successive cycles of association and dissociation at 20°C. The association rate was slow (720 M^{-1} s^{-1}) and the dissociation rate was moderate (1.8×10^{-3} s^{-1}) for protein interaction. A dissociation constant (K_D) of 2.5 (±0.18) μM was obtained from the kinetic constants. A slightly higher K_D of 7.2 μM was obtained when equilibrium between virus and soluble receptor was reached in solution. At 30°C, binding of sICAM-1 disrupted HRV3, as monitored by a loss in resonance units. © 1994 Academic Press, Inc.

Human rhinoviruses are small, nonenveloped RNA viruses of the picornavirus family that cause 40–50% of all cases of common cold. These viruses have a capsid of icosahedral symmetry and are 300 Å in diameter (1, 2). The outer part of the capsid is constructed from 60 copies of viral coat proteins VP1, VP2, and VP3. Viral RNA and viral protein 4 are located inside the proteinaceous capsid. It was proposed that the receptor binding site was located in a depression or "canyon" encircling the 5-fold icosahedral vertices and that five receptor binding sites would be present in each of these vertices (3). Structural and mutational analyses have confirmed these hypotheses (4, 5). The residues implicated in the interaction with the receptor are buried in the "canyon," which make them inaccessible to antibodies and protect the viral receptor binding site from immune surveillance (3).

Intercellular adhesion molecule-1 (ICAM-1) is a cell surface glycoprotein that binds the leukocyte integrins LFA-1 and Mac-1 and promotes a wide variety of cellular interactions (6–9). ICAM-1 also is the receptor for the major group of rhinoviruses (10–12) and for *Plasmodium falciparum*-infected erythrocytes (13, 14).

ICAM-1 contains five immunoglobulin-like extracellular domains (D1–D5), a hydrophobic transmembrane domain, and a short cytoplasmic domain (15, 16). The binding sites for *P. falciparum*-infected erythrocytes, LFA-1, and rhinovirus were localized in the two most external domains of the molecule (D1 and D2) (13, 14, 17). Mac-1 binds to the third domain (9).

A soluble form of ICAM-1 (sICAM-1) comprising the entire extracellular portion of the molecule (D1–D5) binds to rhinovirus in solution and inhibits infection *in vitro* (18). sICAM-1 can also induce irreversible modification of the rhinovirus capsid (disruption), which leads to the release of the RNA and viral proteins and to virus inactivation (19). Chimeric ICAM-1/immunoglobulin molecules showed higher avidity than sICAM-1 for rhinovirus (20). Viral disruption mediated by soluble receptor is pH and temperature dependent (21, 22).

BIAcore is a new technology designed to analyze macromolecular interactions in real time. The interaction between an immobilized molecule in a sensor

1046-2023/94 $6.00

chip and a ligand is monitored by surface plasmon resonance, which detects changes in mass (23). This technology has been used extensively to analyze antigen–antibody interactions, with affinity in the nanomolar range.

We have used BIAcore to analyze the interaction between rhinovirus and sICAM-1, which has affinity in the micromolar range. Specific and reproducible interactions between sICAM-1 and immobilized rhinovirus were obtained, and kinetic and affinity constants determined at 20°C. A moderate dissociation rate constant (k_{diss}), a low association rate constant (k_{ass}), and a dissociation constant (K_D) of 2.5 μM were obtained with this methodology. Slightly higher K_D (7.2 μM) was obtained with another method. Interestingly, at 30°C binding of sICAM-1 caused disruption of the rhinovirus capsid.

MATERIALS AND REAGENTS

Amine coupling kit (Pharmacia Biosensor AB)
- 0.1 M *N*-hydroxysuccinimide (NHS)
- 0.4 M *N*-ethyl *N'*-(dimethylaminopropyl)carbodiimide (EDC)
- 1 M ethanolamine hydrochloride, pH 8.5

BIAcore System Manual, Pharmacia

Buffers
- PBS (pH 7.4): 137 mM NaCl, 2.7 mM KCl, 1.47 mM KH_2PO_4, 4.86 mM Na_2HPO_4, 0.68 mM $CaCl_2$, and 0.49 mM $MgCl_2$, pH 7.4
- PBS (pH 8.0): 137 mM NaCl, 2.7 mM KCl, 1.47 mM KH_2PO_4, 4.86 mM Na_2HPO_4, pH 8.0
- TEA–saline buffer: 50 mM triethylamine, 150 mM NaCl, pH 11.0
- Tris–saline buffer: 10 mM Tris, 150 mM NaCl, pH 8.0

Complete insect cell medium
- Grace's insect cell culture medium (Gibco) supplemented with yeastolate (3.33 g/liter), lactalbumin hydrolysate (3.33 g/liter), and 10% FCS

^{35}S protein labeling mix (NEN)
- [^{35}S]Methionine and cysteine, 1140.0 Ci/mmol

N-Glycanase (Genzyme), 250 units/ml
- Digestion of sICAM-1 with *N*-Glycanase: A solution of 2 mg of sICAM-1/ml in PBS containing 0.5% SDS and 50 mM β-mercaptoethanol is boiled for 5 min. NP-40 is added to a final concentration of 2.5%. Then 0.3 unit of *N*-Glycanse/20 μg of sICAM-1 is added and incubated overnight at 37°C.

Polyclonal rabbit anti-mouse Fcγ (Pharmacia)

METHODS AND RESULTS

sICAM-1

sICAM-1 comprising the entire extracellular portion of the molecule was obtained using a recombinant baculovirus containing the mutant cDNA clone (Y452E/F*) that codes for sICAM-1 (9). *Spodptera frugiperda* (SF9) cells were cultured in suspension with complete insect cell medium at a density of 1 to 2 $\times$ 10^6 cells/ml. High-titer viral stock was obtained by infecting SF9 cells (1.5 $\times$ 10^6 cell/ml) with a multiplicity of infection (moi) of 0.1 plaque forming unit (pfu)/cell. Infectious medium was collected 3–4 days postinfection and kept at 4°C. The titer of the viral stock ($\sim$1.5 $\times$ 10^8 pfu/ml) was determined as described by Summers and Smith (24).

SF9 cells (2 $\times$ 10^6 cells/ml) were infected with recombinant baculovirus at 10 pfu/cell and soluble protein was secreted into the medium. The highest protein concentration in the medium was obtained 96 h postinfection (Fig. 1A). Increasing the moi decreased the time to reach the highest protein concentration and gave a more homogeneous protein (data not shown). Protein was purified by immunoaffinity chromatography on ICAM-1 monoclonal antibody R6.5–Sepharose (20-ml column) from 1 liter of medium collected 96 h postinfection. Medium was run through the column at a flow rate of 0.5 ml/min. After loading, the column was washed with 200 ml of Tris–saline buffer, pH 10.0, and the protein eluted with TEA buffer, pH 11.0. Fractions collected during elution (7 ml) were neutralized with 400 μl of 1 M Tris, pH 6.0. Fractions containing sICAM-1 ($\sim$20 ml) were concentrated up to 2 ml and protein was further purified by size exclusion chromatography on a TSK-Gel G3000SW column equilibrated with PBS (pH 7.4 or 8.0). Highly purified sICAM-1 with a molecular weight around 60 kDa was obtained after these two purification steps (Fig. 1B, lane 1). Electrophoresis showed a broad band, suggestive of species differing in glycosylation. sICAM-1 treated with *N*-Glycanase gave a protein that migrated as a sharp band of 52 kDa (Fig. 1B, lane 2). Oligomannose-containing fucosylated cores are a major part of the glycoproteins obtained in SF9 cells (25, 26).

To calculate the protein concentration, an extinction coefficient of 0.8 ml/mg · cm, which was calculated by the Peptidestructure module of the University of Wisconsin (GCG program), was used. The predicted molecular weight for the unglycosylated protein (49.6 kDa) was used to determine its molarity.

To metabolically label sICAM-1, insect cells infected with recombinant baculovirus (moi = 10) were cultured for 2 days in cysteine and methionine-free medium supplemented with 0.1 mCi/ml of ^{35}S protein labeling mix (NEN). Labeled receptor was purified from the medium as described above.

Virus Obtention and Purification

HRV3 was used in this work because it is known to have a higher affinity than other serotypes for ICAM-1 (19). HRV3 was purified by sucrose gradient sedimentation as described (22). A viral solution (1 ml) containing about 30% sucrose and 0.01% BSA in PBS (pH 7.4) was obtained after the last purification step. To eliminate the BSA and sucrose from the viral stock, the virus solution was diluted 5-fold in PBS (pH 7.4) and viral particles were pelleted by ultracentrifugation for 3 h at 40,000 rpm and 4°C in a Beckman SW55 rotor before resuspension in dilution buffer. Virus concentration was calculated from OD_{260} (1 OD_{260} = 9.4 $\times$ 10^{12} virus/ml) (27). A plaque-forming assay of the viral stock was performed as described by others (28).

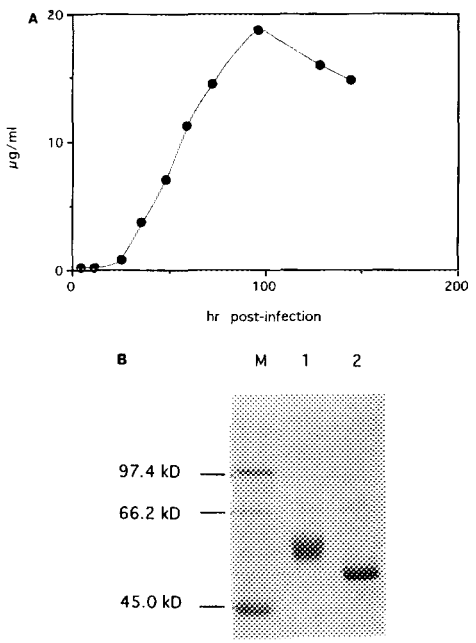

FIG. 1. Time course of protein expression in baculovirus-infected cells. (A) SF9 cells were infected with a recombinant baculovirus that contains the sICAM-1 cDNA at a moi of 10 pfu/cell. Protein concentration in the extracellular medium at different times post-infection was determined by ELISA using baculovirus sICAM-1 as standard. (B) 10% PAGE of purified baculovirus sICAM-1 before (1) and after (2) *N*-glycanase treatment. Marker: M.

The purified virus stock contained approximately 600 virus/pfu.

Rhinovirus Immobilization

The virus was covalently linked to the carboxymethylated dextran on the surface of the chip, and the soluble receptor was injected through the rhinovirus surface. HRV3 was immobilized instead of the receptor because of the lower availability of the virus. HRV3 was covalently immobilized to the dextran surface via primary amino groups, using the Amine Coupling Kit (Pharmacia Biosensor AB). The carboxylate groups on the dextran were activated by injection of 35 μl of NHS/EDC mix (1/1) at 5 μl/min and 20°C prior to virus injection. Purified virus ($\sim$10 μl = 3.7 μg = 2.7 $\times$ 10^{11} viral particles) in PBS (pH 7.4) was diluted with 70 μl

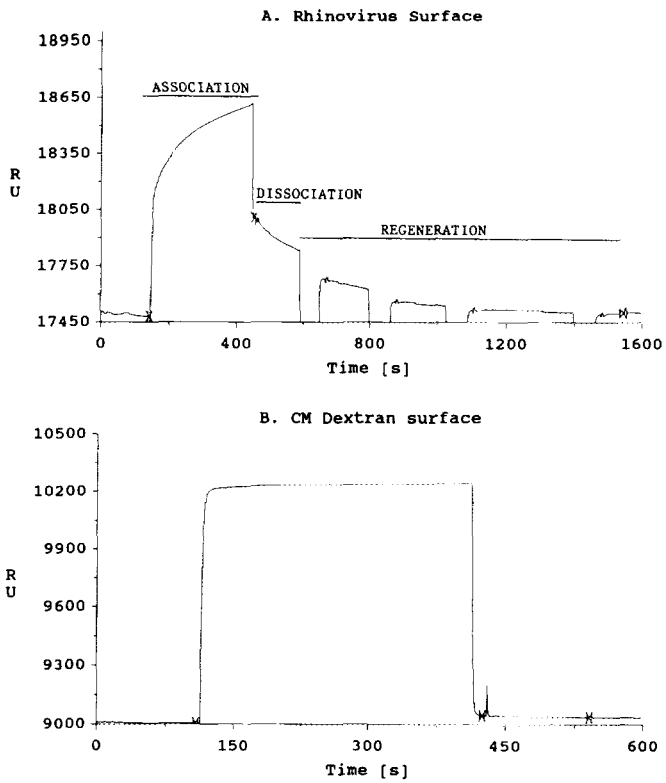

FIG. 2. Sensorgrams obtained from injection of sICAM-1 through rhinovirus and carboxymethyl surfaces. sICAM-1 (5 μM) was injected through carboxymethyl (CM) dextran surfaces with (A) or without immobilized HRV3 (B) at a flow rate of 4 μl/min. Rhinovirus surface was regenerated by 4 pulses of 25 mM Mes buffer, pH 6.0. Association, dissociation, and regeneration phases of the sensorgrams are indicated. Relative responses with respect to the initial baseline after the injection of sICAM-1 (bound) and at the end of each cycle were recorded.

of 10 mM Na acetate, pH 5.7, and 35 μl (1.2×10^{11} viral particles) of this mix was injected through the activated matrix at the same flow and temperature as in the activation step. Acidification of the virus increased its positive charge and led to electrostatic interactions between virus and dextran (data not shown). Coupling of amine groups of the viral coat proteins with the activated esters of the dextran gave virus immobilization. Ethanolamine (35 μl) was injected after virus immobilization to block unreacted *N*-hydroxysuccinimide esters. About 9000 resonance units (RU) of virus was immobilized. This corresponds to 8.0×10^8 viral particles (~0.7% of the total injected), based on 1000 RU per 10 g of protein/liter in the dextran, and the M_r of the virus of 8.16×10^6. Thus, 1000 RU represents about 1.23 μM bound virus.

Acidification of HRV3 was required for immobilization. Acidification of rhinovirus can induce disruption of the viral capsid (29). However, no disruption of HRV3 capsid was observed by sucrose gradient sedimentation analysis after incubation of the virus for 15 min at 20°C in 10 mM Na acetate, pH 5.5 (data not shown). Sucrose gradient sedimentation analysis was performed as described elsewhere (20).

Interaction of sICAM-1 with Rhinovirus

Purified sICAM-1 (5 μM) in PBS (pH 7.4) was injected through the immobilized rhinovirus at a flow

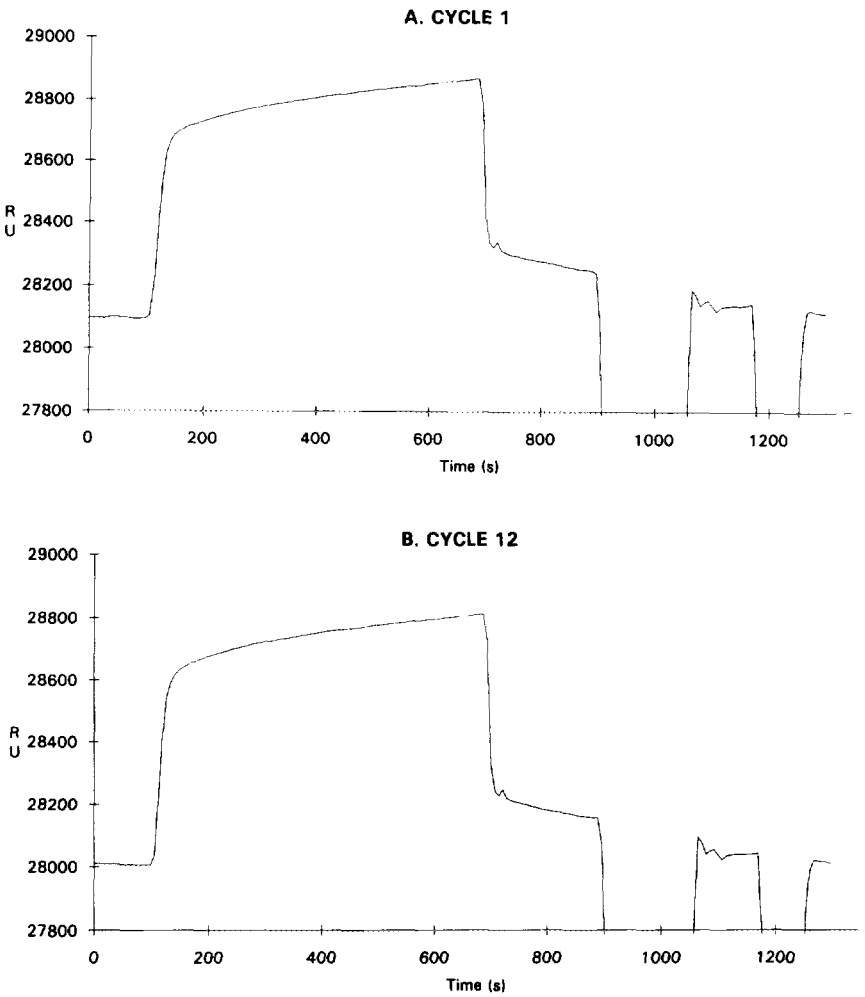

FIG. 3. Integrity of immobilized rhinovirus. 30 μl of sICAM-1 (4 μM) in PBS (pH 7.4) was injected 12 consecutive times at 20°C through a surface containing 18,000 RU of immobilized HRV3. Cycles 1 (A) and 12 (B) are shown. Two pulses (3 and 1 min) of 25 mM Mes buffer, pH 6.0, were selected as regeneration conditions. Relative responses with respect to the initial baseline after the injection of sICAM-1 (bound) and at the end of each cycle were recorded.

rate of 4 μl/min. The profile of the sensorgram recorded during and after the injection of the protein revealed a clear association and dissociation of sICAM-1 (Fig. 2A). The bound sICAM-1 (529 RU) dissociated quickly from the rhinovirus matrix. Regeneration of the surface was achieved by four pulses (1 min) of 25 mM Mes buffer, pH 6.0. Selection of regeneration conditions was based on previous experiments that suggested a decrease in the affinity of sICAM-1 for rhinovirus at lower pH (22).

Injection of sICAM-1 (5 μM) in PBS (pH 7.4) through the carboxymethyl dextran surface with no immobilized virus gave a binding of 41 RU (Fig. 2B), which represented less than 10% of the binding to the rhinovirus surface. Lower nonspecific binding was obtained in later experiments when protein was injected in pH 8.0 PBS instead of pH 7.4 PBS (data not shown).

R6.5 antibody binds to the second domain of ICAM-1 and blocks the interaction of the virus with the receptor (17). Preincubation of sICAM-1 with R6.5 mAb blocked the binding to rhinovirus (sensorgram not shown). Binding was inhibited 85% when sICAM-1 (5 μM) was preincubated with R6.5 (6 μM) for 15 min at 37°C.

Reproducible Interaction of sICAM-1 with the Rhinovirus Surface and Retention of Viral Integrity

Interaction of sICAM-1 with rhinovirus can disrupt the viral capsid and lead to a loss of viral RNA and the capsid protein VP4. The disruption process is highly temperature dependent, and very low disruption is obtained under 30°C (21, 22). Therefore, we analyzed the interaction between virus and receptor in BIAcore at 20°C. The kinetic analysis of rhinovirus–ICAM-1 interaction in BIAcore requires maintenance of an intact virus during the injection of successive sICAM-1 solutions.

To analyze the stability and activity of HRV3 during successive interactions with sICAM-1, 12 consecutive cycles of sICAM-1 binding and regeneration were performed (Fig. 3). sICAM-1 (4 μM) was injected for 10 min through the rhinovirus surface in each cycle. Experiments were performed at 20°C and PBS (pH 7.4) was used as running buffer. Complete regeneration of the surface was achieved by two pulses of 25 mM Mes (3 and 1 min) buffer, pH 6.0, before each sICAM-1 injection. The amount of bound sICAM-1 to the rhinovirus surface in cycles 1 and 12 was 249 and 245 RU, respectively. The bound sICAM-1 was similar in all the injections (265 ± 13.0 RU), which showed that the ability of the immobilized virus to bind ICAM-1 did not change during the experiment. In addition, the virus remained intact during the experiment because no significant decrease of the baseline between cycles 1 and 12 was obtained (−83 RU).

Immobilized rhinovirus also remained intact in a similar experiment at 25°C (not shown). In some cases the integrity of the immobilized virus was preserved for 24 h at 25°C. In other cases, after 24 h at 25°C, sensorgrams similar to sensorgram 2 of Fig. 7 were recorded when sICAM-1 was injected through these surfaces at 25°C (data not shown). No more than 15 cycles

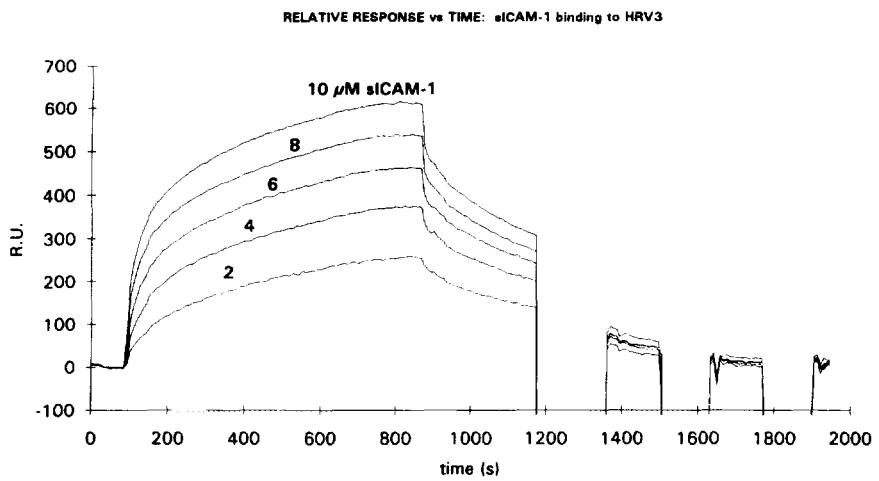

FIG. 4. Overlay plot of sensorgrams obtained from injection of sICAM-1 through rhinovirus surface. 39 μl of 2, 4, 6, 8, and 10 μM sICAM-1 in PBS (pH 8.0) was successively injected through a rhinovirus surface at a flow rate of 3 μl/min and 20°C in this experiment. Surface was regenerated by three pulses (3, 2, and 2 min) of 25 mM Mes buffer, pH 6.0.

of sICAM-1 binding and regeneration were performed on the same rhinovirus surface during the kinetic analysis of the rhinovirus–sICAM-1 interaction.

Determination of Dissociation and Kinetic Constants

Determination of the association and dissociation constants in BIAcore requires successive injections of ligand at different concentrations through the dextran with the immobilized reactant. To analyze the kinetics of the sICAM-1 and rhinovirus interaction, 1 to 10 μM sICAM-1 in PBS (pH 7.4 or 8.0) was injected consecutively through the rhinovirus surface in each experiment at 20°C. The rhinovirus surface was regenerated by three pulses (3, 2, and 2 min) of 25 mM Mes buffer, pH 6.0. The experiments were performed in auto-mode, and sensorgrams obtained for each injection were recorded for kinetic analysis. An overlay plot of the sensorgrams obtained in a typical experiment is presented in Fig. 4. The sensorgrams did not plateau, showing that equilibrium was not reached during the 13-min injection period. The initial and final baseline did not change between the cycles, showing that the rhinovirus surface was stable during the experiment.

Analysis of the Binding Data

Sensorgrams recorded during the interaction of sICAM-1 with the immobilized virus were analyzed by the linear transformation method to obtain the kinetic constants (BIAcore System Manual). Linear analysis of the binding data uses the slope (k_s) of a plot of dR/dt versus R to determine the association constant (k_{ass}) (Table 1, Fig. 5A). The equation

$$k_s = k_{ass}C + k_{diss} \quad [1]$$

TABLE 1

Analysis of the Binding Data: Determination of Kinetic Constants

Analysis of the association phase

Cycle No.	Concn (nM)	k_s	SE	R	From time (s)	To time (s)
1	2,000	0.00382636	0.0015784	0.161657988	200	310
2	4,000	0.00561314	0.00150844	0.267960659	185	275
3	6,000	0.00653272	0.00103388	0.459704943	175	250
4	8,000	0.00840823	0.00123166	0.530490789	170	230
5	10,000	0.01018954	0.00204477	0.514438967	165	200

k_{ass} calculation
0.00225757 intercept (k_{diss})
7.7607*E*-07 slope
0.99502564 coefficient of correlation R
776.072049 k_{ass} (M^{-1} s^{-1})

Analysis of the dissociation phase

Cycle No.	k_{diss}	SE	R	From time (s)	To time (s)
10000.txt	0.00166673	2.1748*E*-05	0.993342141	60	100

Summary

Immobilized ligand	HRV3
Immobilized amount	6000
Conditions	20°C, PBS (pH 8.0)
Analyte	sICAM-1
Analyte concentration range	2–10 μM
Association rate constant (k_{ass})	776.072 (M^{-1} s^{-1})
Dissociation rate constant (k_{diss})	0.001746 (s^{-1})
Affinity constant (K_A)	4.44*E* + 05 (M)
Dissociation constant (K_D)	2.25 (μM)

Note. Time intervals selected for the determination of k_s and k_{diss} are indicated as from time/to time. The selected period for the analysis of k_{diss} corresponds to the time after the dissociation began. k_{diss} obtained from the analysis of the association phase is shown as the intercept (k_{diss}) (Fig. 5B). SE and R represent the standard error and correlation coefficient respectively.

allows determination of k_{ass} from a plot of k_s versus C (Table 1, Fig. 5B). k_{diss} can also be obtained from this plot. Several ligand concentrations are required. The slope was calculated from a different time interval for each sensorgram. The selected times for the determination of k_s were higher than 150 s to avoid discontinuities in the dR/dt vs R plots that occurred between 140 and 150 s in all the sensorgrams. The correlation coefficients (R) obtained in the determination of k_s were not very high, perhaps because of the low affinity interaction. Higher correlation coefficients (>0.8) were obtained in the analysis of the interaction of sICAM-1 with monoclonal antibodies (not shown). However, very high correlation coefficients were obtained in the determination of k_{ass} (~0.99), and highly reproducible results were obtained from different experiments (Table 2).

The portion of the sensorgram that corresponds to the dissociation of sICAM-1 from the rhinovirus surface was analyzed to obtain k_{diss}. The slope of a plot of $\ln(R_1/R_n)$ vs time yields the k_{diss} (Table 1, Fig. 5C). The sensorgram obtained for the higher ligand concentration was analyzed to minimize rebinding during dissociation. Low rebinding would be expected because of the low association rate. The dissociation curves showed two discontinuities at about 20 and 50 s after dissociation began, which did not allow us to use the first minute of the dissociation curve in the analysis. These discontinuities reflected changes in pressure related to the movement of the needle after the injection and can be prevented now by the use of the "kinject" command (BIAcore System Manual). The selected period for the analysis of k_{diss} was from 60 to 100 s after dissociation began (Table 1). Very high (>0.9) correlation coefficients were always obtained in this determination.

Association and dissociation kinetic constants were determined from three independent experiments with different viral surfaces (Table 2). Highly reproducible results were obtained. The dissociation constant (2.5 μM) was obtained from the kinetic constants (Table 2).

The k_{diss} for the interaction of sICAM-1 with rhinovirus (1.8×10^{-3} s^{-1}) was very similar to the k_{diss} obtained with anti-ICAM-1 monoclonal antibodies (Table 3). However, the kinetic rate constant obtained for the association of sICAM-1 to antibodies (3.4×10^4 M^{-1} s^{-1}) was about 50 times higher than that obtained with HRV3. The low k_{ass} may correlate with a low accessibility of the receptor binding site in the virus, which is located in a depression of the viral capsid.

Association and dissociation constants can be also obtained from a Scatchard plot using the amount of ligand bound to the surface at equilibrium. Although no equilibrium state was reached in these experiments, we used the data of sICAM-1 bound to determine the dissociation constant (K_D) with the equation

$$R_b/C = (R_{max}/K_D) - (R_b/K_D) \quad [2]$$

where R_b is the specific bound sICAM-1, C the concentration of sICAM-1, K_D the dissociation constant, and R_{max} the maximum amount of sICAM-1 that can be bound to the surface (BIAcore System Manual, pp. 8–12). A K_D of 4.0 μM was obtained from this analysis.

A biphasic curve was obtained from the representation of R_b/C versus R_b when 1 to 10 μM sICAM-1 was injected as described in Fig. 4 (Fig. 6A). Biphasic curves in Scatchard plots can be related to the presence of more than one class of sites (30).

TABLE 2

Kinetic and Dissociation Constants

Expt	ICAM-1 (μM)	k_{ass} (M^{-1} s^{-1})	$k_{diss} \times 10^3$ (s^{-1})	K_D (μM)	K'_D (μM)
1	1, 2, 4, 6, 8, 10	776.07	1.746	2.25	4.0
2	2, 4, 6, 8	739.11	1.871	2.50	1.8
3	2, 4, 6, 8, 10	637.25	1.75	2.70	6.3
Average		717.5 (58.7)	1.8 (0.58)	2.50 (0.18)	4.0 (2.2)

Note. Association (k_{ass}) and dissociation (k_{diss}) kinetic constants and dissociation constants (K_D) from three different experiments are shown. K_D was obtained from the kinetic constants, and K'_D from Scatchard plot using the amount of ICAM-1 bound at the end of each injection. No equilibrium was reached at the end of the injection. K'_D is the average of the two dissociation constants obtained in the biphasic plot (Fig. 6A). Standard deviation is given in parentheses.

The biphasic curve obtained in BIAcore could be related to some heterogeneity in the accessibility of the virus to sICAM-1. Viral particles located inside the carboxymethylated dextran could be less accessible to the soluble receptor than those located in the outer part of the dextran. It could be also possible that small differences in the affinity between virus binding sites were detected in BIAcore. There are a total of 60 sICAM-1 binding sites per virion, and the 5 receptor binding sites encircling the 5-fold vertices of the viral capsid are particularly close. Binding of sICAM-1 to the virus could decrease accessibility for binding of further sICAM-1 molecules.

Affinity of sICAM-1 for Rhinovirus in Solution

The dissociation constant was also obtained from experiments in which HRV3 and [^{35}S]methionine–cysteine labeled receptor were incubated in solution, and virus with bound receptor was separated from free receptor by ultracentrifugation (22). The relation between the radioactivity that co-sedimented with the virus and the input was calculated as the bound/free sICAM-1 ratio. The bound sICAM-1 varied from 2.9 to 5.5% of the input. A K_D of 7.2 μM was determined from the Scatchard plot (Fig. 6B). A good linearity was obtained in the plot. The number of binding sites/virus calculated from the Scatchard was 67, compared to the value of 60 sites/virus theoretically expected.

The K_D obtained in the experiments in which equilibrium was reached in solution was slightly higher than that obtained from the kinetic constants in BIAcore. The biphasic plot obtained from the BIAcore data suggested small differences in the accessibility or affinity of the virus binding sites. The kinetic constants were obtained in BIAcore from the analysis of the first 5 min of the interaction. Thus, association of sICAM-1 with the most accessible sites would be analyzed for k_{ass}, and dissociation data would be for the most rapidly dissociating sites. On the other hand, BIAcore can be considered a heterogeneous system because one of the reactants is immobilized in a solid phase. Higher association constants (lower K_D) have been obtained in heterogeneous than in homogeneous antigen–antibody binding tests (31, 32), which can be explained by differences in kinetic rates between these two systems (32).

Disruption of Rhinovirus by sICAM-1

We showed in Fig. 3 that the integrity of the immobilized virus in BIAcore was preserved after at least

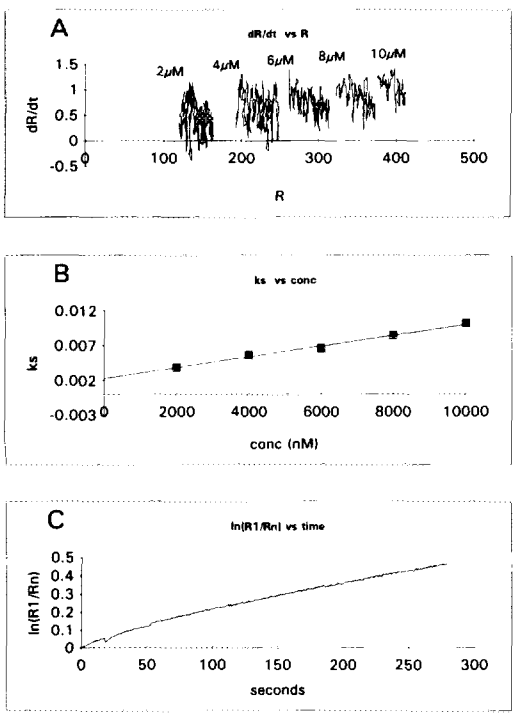

FIG. 5. Analysis of the binding data. (A) dR/dt versus R plots obtained for the sensorgrams presented in Fig. 4. sICAM-1 concentration is indicated. (B) Slopes of the plots presented in A (k_s) were plotted versus sICAM-1 concentration and curves obtained by linear regression. Slope (k_{ass}) and interception with the Y axis (k_{diss}) are shown in Table 1. (C) Plot obtained from the analysis of the dissociation phase of the sensorgram corresponding to 10 μM sICAM-1 presented in Fig. 4.

TABLE 3

Interaction of sICAM-1 with Anti-ICAM-1 Monoclonal Antibodies: Kinetic and Dissociation Constants

Antibody	k_{ass} (M^{-1} s^{-1})	$k_{diss} \times 10^3$ (s^{-1})	K_D (nM)
R6.5	23,748	2.15	90.0
LB2	36,445	1.867	51.2
RR1/1	40,348	1.864	46.0
Average	33,514	1.96	62.4

Note. Kinetic and dissociation constants were calculated in BIAcore. A polyclonal rabbit anti-mouse Fcγ antibody (Pharmacia) was immobilized in the dextran using the amine coupling kit as recommended by the manufacturer. Anti-ICAM-1 monoclonals (32 μl, 20 μg/ml) and sICAM-1 (36 μl) were consecutively injected through the surface containing the rabbit antibody at 4 μl/min and 25°C. Surface was regenerated by injection of 8 μl of 100 mM HCl after each cycle. 50, 100, 150, 200, 250, and 300 nM sICAM-1 were injected in these experiments and kinetic and dissociation constants determined as described in Table 1. Monoclonals antibodies recognize domains 1 and 2 of ICAM-1 (14).

12 successive injections of sICAM-1 at 20°C. The integrity of the virus was also maintained at 25°C. However, the injection of high but not low concentrations of sICAM-1 at 30°C gave sensorgrams consistent with the disruption of immobilized rhinovirus (Fig. 7).

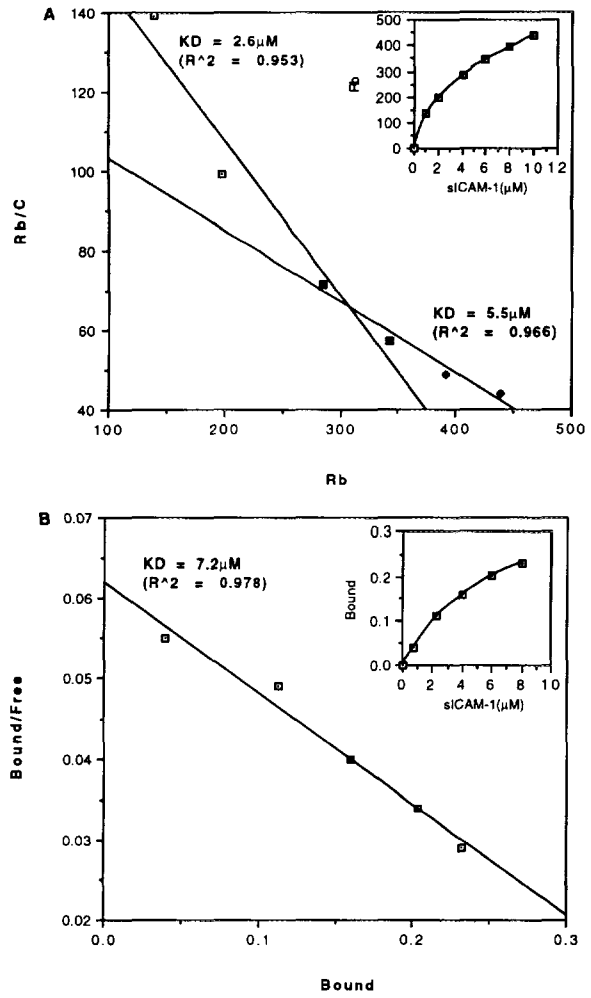

FIG. 6. Scatchard plots from the binding of sICAM-1 to rhinovirus. (A) 39 μl of 1, 2, 4, 6, 8, and 10 μM sICAM-1 was injected through a surface with or without virus, and the RU after the injection was recorded as total and unspecific bound, respectively. Injections were made at 20°C and a flow rate of 3 μl/min. Specific binding (R_b) was obtained by subtracting the unspecific RU from the total RU. Inset: R_b (RU) obtained in each injection. (B) HRV3 (4×10^9 virus/μl) was incubated with varying amounts of sICAM-1 (0.75, 2.3, 4, 6, and 8 μM) for 60 min at 20°C. Cold and [^{35}S]methionine–cysteine-labeled sICAM-1 were used in these experiments. Samples (25 μl) were ice cold and sedimented through a 1-ml 5–30% sucrose gradient for 1 h at 40,000 rpm and 4°C in a Beckmann SW55 rotor. Fractions were collected from the bottom and scintillation counted. The relation between the radioactivity that cosedimented with the virus and the input was calculated as the bound/free sICAM-1 ratio, and K_D was determined from the slope of the plot. Inset: Bound sICAM-1 (μM) versus input one. Bound sICAM-1 was 0.040, 0.113, 0.160, 0.204, and 0.232 μM.

Injection of 1 μM sICAM-1 at 30°C yielded sensorgrams similar to those obtained at 20°C, and no decrease of the baseline was obtained after regeneration of the surface (Fig. 7, Table 4). However, the injection of 2 and 4 μM sICAM-1 gave sensorgrams on which the recorded RU increased and then decreased during the injection. The baseline also decreased after regeneration of the surface. Injection of 6 and 8 μM sICAM-1 gave sensorgrams on which the response increased during the injection phase, but a decrease in the baseline occurred after these injections (Table 4).

The disruption of rhinovirus causes the release of RNA and VP4 and decreases the affinity of the virus for the receptor (19, 22). Thus, disruption of the virus in the matrix would decrease the RU as a result of the release of virus mass. The decrease in RU during the injection phase in sensorgrams 2 and 3 (Fig. 7) suggests that disruption of the immobilized rhinovirus occurs during the interaction with sICAM-1.

sICAM-1 still bound to the rhinovirus surface at 6 and 8 μM, although the amount of bound material was lower than that obtained at 1 μM with native virus (Table 4). Whether sICAM-1 bound to native or disrupted virus in these experiments is not clear, because both were probably present in the matrix. The decrease in the baseline in these cases appears to be related to disruption of the virus that occurred during injection and was masked by sICAM-1 binding, because a low number of resonance units are already apparent at the end of the dissociation phase, before the pH 6.0 wash began.

TABLE 4

Rhinovirus–sICAM-1 Interaction at 30°C

Sensorgram	sICAM-1 (μM)	Bound (RU)	Rel. resp (end)
1	1	467	8
2	2	421	−126
3	4	221	−379
4	6	318	−224
5	8	330	−175

Note. The data were obtained from sensorgrams presented in Fig. 7. Bound sICAM-1 is measured as the difference in RU between the beginning and the end of the injection. The difference in the signal between the end and the beginning of each cycle is shown as Rel. resp.

We determined that about 10 sICAM-1 molecules were bound to each viral particle during the disruption in sensorgram 2. These data were determined from the amount bound at the top of the sensorgram (512 RU), which corresponds to a sICAM-1 concentration of 87.0 μM (1000 RU = 167.0 μM sICAM-1). By contrast, disruption did not occur in sensorgram 1, in which the sICAM-1 binding reached 467 RU by the end of the injection. The rhinovirus surface contained 7246 RU, representing a virus concentration of 8.9 μM. This determination could overestimate the number of binding sites on the surface because some of these sites could be inaccessible after the immobilization. Experimental determination of the number of binding sites is required to obtain a more accurate quantitation of the number of receptors bound to the virus during disruption.

CONCLUSION

We have used BIAcore to determine the affinity and kinetic constants for the interaction of sICAM-1 with rhinovirus serotype 3. Highly reproducible results were obtained with this methodology, and the virus remained stable during the interaction with the receptor at 20°C. We show that this is a low-affinity interaction, with a dissociation constant in the micromolar range. When sICAM-1 binding to HRV3 is compared to that to antibodies, the association rate for HRV3 is much lower but the dissociation rate is comparable. This may be related to the inaccessibility of the binding site in the rhinovirus canyon or the necessity for a conformational change, or it may be fortuitous.

The analysis of the interaction in BIAcore has given a lower K_D and a different Scatchard plot than equi-

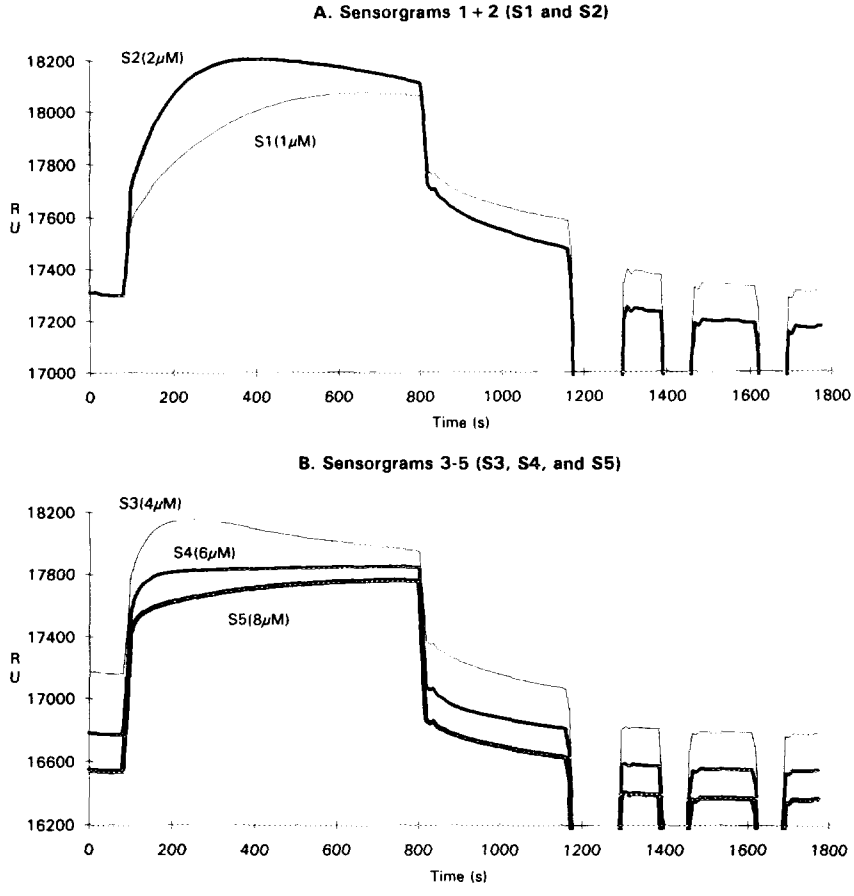

FIG. 7. Rhinovirus disruption in BIAcore. 1, 2, 4, 6, and 8 μM sICAM-1 in PBS (pH 8.0) were successively injected through a rhinovirus surface at 30°C and 3 μl/min. Sensorgrams recorded for the injection of 1 to 8 μM sICAM-1 were labeled as S1 to S5, respectively. Concentrations of sICAM-1 injected are given in parentheses.

librium measurements in solution. We have speculated that there may be small differences in the accessibility of the binding sites related to the degree of occupancy, which correlates with a biphasic plot. The initial minutes of the interaction were analyzed in the determination of the kinetic constants. Interaction of sICAM-1 with the most accessible sites would occur in the initial moments of the interaction, and sites from which dissociation is more rapid would also be selectively measured in the dissociation phase. On the other hand, one of the reactants is immobilized in BIAcore, which could give rate constants in this system different from those obtained in solution (32).

Modification of the viral structure during the interaction with sICAM-1 was also detected in BIAcore, which showed that this methodology can be used to detect changes in subunit association states within macromolecular assemblies that occur as a result of biospecific interactions.

ACKNOWLEDGMENTS

This work was supported by NIH Grant AI31921. José M. Casasnovas was a fellow of the Human Frontiers in Science Program.

REFERENCES

1. Rossmann, M. G., Arnold, E., Erickson, J. W., Frankenberger, E. A., Griffith, J. P., Hecht, H. J., Johnson, J. E., Kamer, G., Luo, M., Mosser, A. G., Ruecker, R. R., Sherry, B., and Vriend, G. (1985) *Nature* **317,** 145–153.
2. Kim, S., Smith, T. J., Chapman, M. S., Rossmann, M. G., Pevear, D. C., Dutko, F. J., Felock, P. J., Diana, G. D., and McKinlay, M. A. (1989) *J. Mol. Biol.* **210,** 91–111.
3. Rossmann, M. G. (1989) *J. Biol. Chem.* **264,** 14587–14590.
4. Olson, N. H., Kolatkar, P. R., Oliveira, M. A., Cheng, R. H., Greve, J. M., McClelland, A., Baker, T. S., and Rossman, M. G. (1993) *Proc. Natl. Acad. Sci. USA* **90,** 507–511.
5. Colonno, R. J., Condra, J. H., Mizutani, S., Callahan, P. L., Davies, M. E., and Murcko, M. A. (1988) *Proc. Natl. Acad. Sci. USA* **85,** 5449–5453.
6. Marlin, S. D., and Springer, T. A. (1987) *Cell* **51,** 813–819.
7. Kishimoto, T. K., Larson, R. S., Corbi, A. L., Dustin, M. L., Staunton, D. E., and Springer, T. A. (1989) *Adv. Immunol.* **46,** 149–182.
8. Dustin, M. L., and Springer, T. A. (1988) *J. Cell Biol.* **107,** 321–331.
9. Diamond, M. S., Staunton, D. E., Marlin, S. D., and Springer, T. A. (1991) *Cell* **65,** 961–971.
10. Greve, J. M., Davis, G., Meyer, A. M., Forte, C. P., Yost, S. C., Marlor, C. W., Kamarck, M. E., and McClelland, A. (1989) *Cell* **56,** 839–847.
11. Staunton, D. E., Merluzzi, V. J., Rothlein, R., Barton, R., Marlin, S. D., and Springer, T. A. (1989) *Cell* **56,** 849–853.
12. Tomassini, J. E., Graham, D., DeWitt, C. M., Lineberger, D. W., Rodkey, J. A., and Colonno, R. J. (1989) *Proc. Natl. Acad. Sci. USA* **86,** 4907–4911.
13. Ockenhouse, C. F., Betageri, R., Springer, T. A., and Staunton, D. E. (1992) *Cell* **68,** 63–69.
14. Berendt, A. R., McDowall, A., Craig, A. G., Bates, P. A., Sternberg, M. J. E., Marsh, K., Newbold, C. I., and Hogg, K. (1992) *Cell* **68,** 71–81.
15. Simmons, D., Makgoba, M. W., and Seed, B. (1988) *Nature* **331,** 624–627.
16. Staunton, D. E., Marlin, S. D., Stratowa, C., Dustin, M. L., and Springer, T. A. (1988) *Cell* **52,** 925–933.
17. Staunton, D. E., Dustin, M. L., Erickson, H. P., and Springer, T. A. (1990) *Cell* **61,** 243–254.
18. Marlin, S. D., Staunton, D. E., Springer, T. A., Stratowa, C., Sommergruber, W., and Merluzzi, V. (1990) *Nature* **344,** 70–72.
19. Greve, J. M., Forte, C. P., Marlor, C. W., Meyer, A. M., Hoover-Litty, H., Wunderlich, D., and McClelland, A. (1991) *J. Virol.* **65,** 6015–6023.
20. Martin, S., Casasnovas, J. M., Staunton, D. E., and Springer, T. A. (1993) *J. Virol.* **67,** 3561–3568.
21. Hoover-Litty, H., and Greve, J. M. (1993) *J. Virol.* **67,** 390–397.
22. Casasnovas, J. M., and Springer, T. A. (1993) Submitted for publication.
23. Malmqvist, M. (1993) *Nature* **361,** 186–187.
24. Summers, M. D., and Smith, G. E. (1987) A Manual of Methods for Baculovirus Vectors and Insect Cell Culture Procedures, Texas Agricultural Experimental Station.
25. Luckow, V. A., and Summers, M. D. (1988) *Biotechnology* **6,** 47–55.
26. Butters, T. D., Jones, I., Clarke, V. A., and Jacob, G. S. (1991) *Glycoconjugate J.* **8,** 240.
27. Rueckert, R. R., and Pallansch, M. A. (1981) *Methods Enzymol.* **78,** 315–325.
28. Sherry, B., and Rueckert, R. (1985) *J. Virol.* **53,** 137–143.
29. Rueckert, R. R. (1990) *in* Virology (Fields, B. N., Knipe, D. M., Chanock, R. M., Hirsch, M. S., Melnick, J. L., Monath, T. P., and Roizman, B., Eds.), Vol. 2, pp. 507–548, Raven Press, New York.
30. Cantor, C. R., and Schimmel, P. R. (1980) Biophysical Chemistry, pp. 856–859, Freeman, San Francisco.
31. Nygren, H., Kaartinen, M., and Steuberg, M. (1986) *J. Immunol. Methods* **92,** 219–225.
32. Azimzadeh, A., Pelleguer, J. L., and Van Rejenmortel, M. H. V. (1992) *J. Mol. Recogn.* **5,** 9–18.